Two-degree-of-freedom Robust Feedback Control of a Sliding Gate Automation

Daniel Cunico, Angelo Cenedese, Luca Zaccarian, Mauro Borgo

Fig. 1. The electric gate used for the experimental tests.

Two-degree-of-freedom Robust Feedback Control of a Sliding Gate Automation

Daniel Cunico and Angelo Cenedese
Department of Information Engineering
University of Padova, Padova, Italy
daniel.cunico@phd.unipd.it
angelo.cenedese@unipd.it

Luca Zaccarian
LAAS-CNRS, Université de Toulouse, Toulouse, France and
University of Trento, Italy
zaccarian@laas.fr

Mauro Borgo
BFT SpA
Vicenza, Italy
mauro.borgo@bft-automation.com

Abstract

A control strategy consisting of a feedforward action and a robust feedback for a gate automation is presented, where a low-cost and non-regenerative motor drive is used. A model of the system is developed and feedback linearization is used to compensate for the highly nonlinear dynamics of the electric drive. To achieve good motion tracking performance we design a smooth reference associated with a feedforward action, based on the nominal model of the system. In addition, based on a model of the uncertainties a robust feedback controller is tuned by solving a set of linear matrix inequalities, combining the optimization of a LQR cost with some pole placement constraints. Finally, we test the proposed control strategy on an experimental device, obtaining satisfactory results.

Index Terms

Industrial Motion Control, Trajectory Tracking, Robust Control, Linear Matrix Inequalities.

I. Introduction

Access automation systems are widely used to restrict the entry of vehicles into a property or to manage the access of people in a building. In this sector, the industries need to provide products with excellent performance, but at the same time they must have low production costs. These devices can be considered as typical electromechanical motion systems [1] consisting of an electric motor that moves a load at the desired speed through a mechanical transmission, while their control system must be simple enough to be implemented on embedded hardware with limited computational capacity. The control architecture is usually divided in two hierarchical levels [2], [3]. A motion planner generates the desired reference based on the parameters set by the user, while a feedback controller minimizes the deviation of the actual trajectory from the desired reference.

In this paper, we consider the control design of an automatic electric gate, a common access automation system shown in Fig. 1. Due to manufacturing costs, non-regenerative DC drives [4], [5] are usually used to command the motor, which cannot generate a controlled braking torque because they only operate in two quadrants. Furthermore, the dynamics of these drives can be highly nonlinear, increasing the difficulties in the design of the control system. Following [6], we illustrate the dynamics of the electric drive and we employ feedback linearization to compensate its nonlinear effects. We design a polynomial motion reference to be tracked by the feedback controller and defined as a function of the user requirements. Jerk limitation in the trajectory planning is introduced since it provides a means to limit the variation rate of the actuator torques [7] and is of great relevance in reducing the structure vibrations, wear on the machinery and positioning error during the movement [8]–[10]. The main control goal is to obtain good tracking performance and a smooth maneuver, considering that the controller should be robust with respect to possible slow unmodeled dynamics, small delays in the feedback loop and quantization effects. The control law is defined as the sum of a feedforward action, computed on the basis of a nominal model, and a robust feedback term that takes into account model uncertainties, e.g. coming from the load inertia. The feedback controller synthesis is formulated as a linear matrix inequality (LMI) optimization problem [11]. This numerical approach has several advantages.

Indeed it is possible to take into account a wide range of plant parameters occurring at different operating points, resulting in robust stability of the gate automation. In addition, the LMI constraints allow us to solve a linear quadratic regulator (LQR) problem [12], [13] and to shape the performance specifications constraining the eigenvalues of the closed-loop system in a desired region of the left half-plane [14].

The paper is organized as follows. Section II introduces the mechanical system model, the identification procedure and the electrical drive with the feedback linearization technique. Section III presents the proposed control method together with the reference generation and feedforward action, while the robust feedback control is design in Section IV. Experimental results are shown in Section V, followed by conclusions in Section VI. For reasons of confidentiality, all the units of measure are normalized and the technological details are omitted. However, this does not affect the contribution of the work, which is fully parametric and can be implemented on any similar electromechanical system, thereby making our control technique broadly applicable and easily reproducible.

II. System Model

The electric gate application can be schematized as shown in Fig. 2. The input of the system is the duty cycle of a PWM signal δ that controls the voltage u_a supplied to the motor. The DC motor exerts the torque τ_m on the mechanical subsystem through a gearbox, allowing the gate to move with a desired linear speed $v(t)$. The mechanical system is illustrated in Fig. 3. In the following, a model of the system is presented. The electrical equation of a DC motor [15] is:

$$u_\mathrm{a}(t) = R_\mathrm{a} i_\mathrm{a}(t) + L_\mathrm{a}\frac{di_\mathrm{a}(t)}{dt} + e_\mathrm{a}(t), \tag{1}$$

where $u_a(t)$ is the terminal voltage, $i_a(t)$ is the armature current, R_a is the winding resistance, L_a is the inductance and $e_a(t)$ is the back electromotive force (BEMF). Denoting by ω_m the mechanical speed of the motor, the BEMF and the torque exerted at the motor shaft correspond to

$$e_\mathrm{a}(t) = k_\mathrm{t}\omega_\mathrm{m}(t), \quad \tau_\mathrm{m}(t) = k_\mathrm{t} i_\mathrm{a}(t), \tag{2}$$

where k_t is the torque constant. Because of the power balance between the input electrical power and the output mechanical power, the two constants in eq. (2) coincide. The motor is connected to the load by a two-stage transmission, considered to be rigid: a worm gear reducer connected to a pinion and a rack actuator. The mechanical equation of the system is

$$\tau_\mathrm{m}(t) = J_\mathrm{m}\frac{d\omega_\mathrm{m}(t)}{dt} + b_\mathrm{m}\omega_\mathrm{m}(t) + \tau_\mathrm{p}(t) + \tau_\mathrm{d}(t). \tag{3}$$

where τ_p is the pinion-related torque, τ_d accounts for the Coulomb friction affecting of the mechanical transmission and J_m, b_m are the motor inertia and viscous friction coefficients. Denoting by ω_p the speed of the pinion, we have that:

$$\begin{aligned} \omega_\mathrm{p} = \frac{N_\mathrm{g}}{N_\mathrm{w}}\omega_\mathrm{m} = n_1\omega_\mathrm{m}, \quad \tau_\mathrm{p} = \frac{n_1}{\eta_1}\tau_p', \\ \tau_\mathrm{p}'(t) = J_\mathrm{p}\frac{d\omega_\mathrm{p}(t)}{dt} + b_\mathrm{p}\omega_\mathrm{p}(t) + \tau_\ell(t), \end{aligned} \tag{4}$$

where N_g is the number of teeth in the gear, N_w is the number of threads in the worm, n_1 is the worm gear ratio, $\eta_1 < 1$ is the first gear transmission efficiency, τ_ℓ is the load side torque, J_p and b_p are the pinion inertia and friction, respectively. In a similar way, denoting by $v(t)$ the gate linear speed, we have

$$\begin{aligned} v = r_\mathrm{p}\omega_\mathrm{p} = n_2\omega_\mathrm{p} \Longrightarrow n_2 = \frac{v}{\omega_\mathrm{p}} = r_\mathrm{p}, \quad \tau_\ell = \frac{n_2}{\eta_2}\tau_\ell', \\ \tau_\ell'(t) = m\frac{dv(t)}{dt} + bv(t), \end{aligned} \tag{5}$$

where r_p is the pinion radius, n_2, η_2 are the ratio and the efficiency of the rack and pinion transmission, m and b are the load mass and viscous friction. Note that the rack and pinion gears convert the rotational motion into a linear one. By combining (3)–(5) the overall mechanical system equation is obtained as

$$\begin{aligned} \tau_\mathrm{m}(t) = J_\mathrm{tot}\frac{d\omega_\mathrm{m}(t)}{dt} + b_\mathrm{tot}\omega_\mathrm{m}(t) + \tau_\mathrm{c}\mathrm{sign}(\omega_\mathrm{m}(t)), \\ J_\mathrm{tot} = J_\mathrm{m} + J_\mathrm{p}\frac{n_1^2}{\eta_1} + m\frac{n_1^2 n_2^2}{\eta_1\eta_2}, \\ b_\mathrm{tot} = b_\mathrm{m} + b_\mathrm{p}\frac{n_1^2}{\eta_1} + b\frac{n_1^2 n_2^2}{\eta_1\eta_2}, \end{aligned} \tag{6}$$

with the non-smooth term $\tau_\mathrm{d} = \tau_c\mathrm{sign}(\omega_m)$.

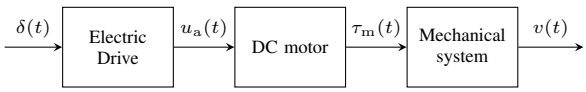

Fig. 2. Electric gate system blocks scheme.

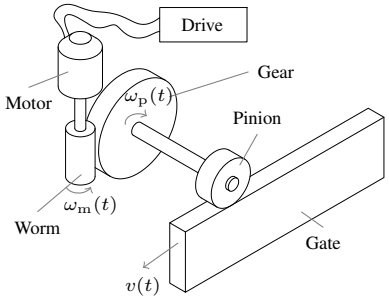

Fig. 3. Scheme of the mechanical system of the gate automation.

To estimate the model parameters we perform a set of experiments with an independent laboratory acquisition system to collect data under sufficient excitation conditions. For identification purposes, a National Instruments DAQ (USB-6216) has been used to acquire the data with a 16-bit ADC resolution and with a 12-bit resolution encoder (Eltra ER38F) mounted on the motor. The torque constant $k_{\rm t}$ can be estimated from the first equation in (2) by connecting the motor to a differential voltage probe and by mechanically coupling the motor to another one. Controlling the motor at different speeds, the value of $k_{\rm t}$ is then obtained from $u_a = k_{\rm t}\omega_{\rm m}$ (from (1) and (2)) with a linear least squares estimate of the collected BEMF and speed data. The remaining parameters are estimated following the procedure used in [6, eq. (11)-(12)] by acquiring voltage, current and speed signals after imposing constant acceleration/deceleration phases to the motor during the data collection experiment.

A complete and detailed description of the motor drive dynamics is given in [6, Section V], from which the main result concerning the feedback linearization of the electrical dynamics is briefly explained in the following. The driver is composed by a Graetz bridge that rectifies the alternating voltage source $V_{\rm ac}$, and the motor is controlled by chopping the non-negative semi-sinusoids v_+ and thus modifying the average voltage output depending on the firing angle of the switch. The equation that describes the average voltage $\bar{u}_{\rm a}$ during a period T of the drive is given by

$$\bar{u}_{\rm a}(\delta, e_{\rm a}) = e_{\rm a}(1-\delta) + \frac{\sqrt{2}V_{\rm ac}}{\pi}(1-\cos(\pi\delta)), \tag{7}$$

where the first term is the weighted contribution of $\bar{u}_{\rm a}(\delta, e_{\rm a})$ during the "off" phase, while the weighted contribution in the "on" phase is given by the semi-sinusoid v_+ with amplitude $\sqrt{2}V_{\rm ac}$ and period T, as per the second term.

By adopting a feedback linearization approach, the objective is to select the duty cycle δ so that the plant seen by the controller is linear. However, function (7) is only invertible in a range depending on $e_{\rm a}$ and, specifically, it depends on the minimum $\bar{u}_{\rm a,m}(e_{\rm a})$ and maximum $\bar{u}_{\rm a,M}(e_{\rm a})$ values of $\bar{u}_{\rm a}$ attainable by choosing $\delta \in [0,1]$. From [6, Proposition 1] by using a feedback linearization approach, we have that for any $u \in [\bar{u}_{\rm a,m}(e_{\rm a}),\ \bar{u}_{\rm a,M}(e_{\rm a})]$, selecting the duty cycle δ as

$$\delta = \delta_{\rm m}(e_{\rm a}) + \frac{1-2\delta_{\rm m}(e_{\rm a})}{\pi}\text{acos}\left(1 - \frac{2(u-\bar{u}_{\rm a,m}(e_{\rm a}))}{\bar{u}_{\rm a,M}(e_{\rm a}) - \bar{u}_{\rm a,m}(e_{\rm a})}\right) \tag{8}$$

the resulting average input obtained from (7) is $\bar{u}_{\rm a}(\delta, e_{\rm a}) = u + \psi$ with $|\psi| \leq 0.01001(\bar{u}_{\rm a,M}(e_{\rm a}) - \bar{u}_{\rm a,m}(e_{\rm a}))$. The values of δ producing the minimum and maximum voltage in (7) are given by [6, eq. (15)]

$$\begin{aligned} \delta_{\rm m}(e_{\rm a}) &= \frac{1}{\pi}\text{arcsin}\left(\frac{e_{\rm a}}{\sqrt{2}V_{\rm ac}}\right) \in \left[0,\ \frac{1}{2}\right), \\ \delta_{\rm M}(e_{\rm a}) &= 1 - \delta_{\rm m}(e_{\rm a}) \in \left(\frac{1}{2},\ 1\right], \end{aligned} \tag{9}$$

and the corresponding voltages are, respectively, [6, eq. (16)]

$$\begin{aligned} \bar{u}_{\rm a,m}(e_{\rm a}) &= \sqrt{2}V_{\rm ac}\left[(1-\delta_{\rm m})\text{sin}(\pi\delta_{\rm m}) + \frac{1}{\pi} - \frac{\cos(\pi\delta_{\rm m})}{\pi}\right], \\ \bar{u}_{\rm a,M}(e_{\rm a}) &= \sqrt{2}V_{\rm ac}\left[\delta_{\rm m}\text{sin}(\pi\delta_{\rm m}) + \frac{1}{\pi} + \frac{\cos(\pi\delta_{\rm m})}{\pi}\right]. \end{aligned} \tag{10}$$

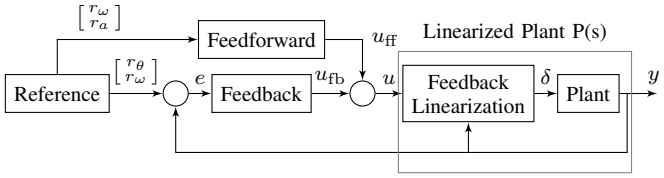

Fig. 4. Two-degree-of-freedom control system diagram.

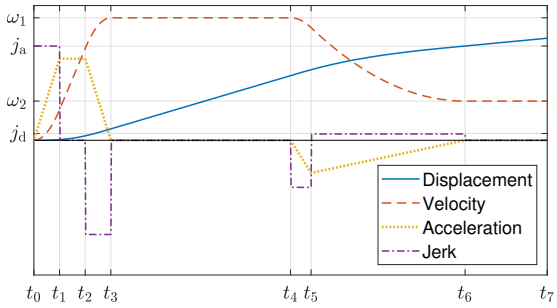

Fig. 5. Polynomial motion reference.

Therefore, by selecting δ as in (8), it results that the error between the requested input u and the applied input $\bar{u}_{\mathrm{a}}$ is only about one percent of the input range.

III. Two-degree-of-freedom control design

In this section we describe a two degree-of-freedom control design that combines a feedforward control and a robust feedback to achieve the desired tracking performance of the automatic gate. The control system architecture is shown in Fig. 4. The reference is generated by polynomial functions in order to obtain a smooth trajectory. The feedback block in Fig. 4 consists of a PI controller tuned with an LMI optimization approach discussed in Section IV. The overall control law u, used to compute δ from the feedback linearizing law (8), is given by the sum of two terms $u(t) = u_{\mathrm{ff}}(t)+u_{\mathrm{fb}}(t)$, where u_{ff} is the feedforward input associated with the reference motion r and u_{fb} is the error feedback stabilizer exploiting the plant measurement $y = [y_\theta \;\; y_\omega]^\top$ corresponding to the mechanical variables. The linearized plant model, given by eqs. (1), (6), has been identified in Section II. Due to eq. (8), the dynamics from u to $\bar{u}_{\mathrm{a}}$ is almost an identity (with a 1% error) when $u \in [\bar{u}_{\mathrm{a,m}}(e_{\mathrm{a}}),\ \bar{u}_{\mathrm{a,M}}(e_{\mathrm{a}})]$. In the following the reference and feedforward blocks of Fig. 4 are discussed.

A polynomial motion reference is designed where jerk constraints are introduced in the trajectory planning to limit the variation rate of the actuator torques. In access automation applications, the reference is usually customized by the user according to the different gate installations that may arise, and consists of four main sections: acceleration, constant high speed, deceleration and constant low speed phases. The last section is needed to comply with safety regulations, requiring that a certain final space θ_{f} of the total displacement is traveled at low speed, to avoid dangerous impacts. As shown in Fig. 5, the motion profile $r(t)$ consists of seven segments, among which the first three constitute the acceleration stage, while the last three represent the deceleration and low speed phases, respectively. The reference must be parametric and computed online based on the following values set by the user: the high ω_1 and low ω_2 velocities, the acceleration time t_{a} and the deceleration time t_{d}. Recall that the motor torque in (6) cannot be negative, namely $\tau_{\mathrm{m}} \geq 0$, since the drive is non-regenerative and it cannot generate a controlled braking torque. Therefore a long enough deceleration phase is needed. The corresponding time evolution of the variables, depicted in Fig. 5, is described for each segment by a set of polynomials and can be deduced from the differential relationship among position θ_{m}, velocity ω_{m}, acceleration a_{m} and jerk j_{m} of the motor:

$$\theta_{\mathrm{m,i}}(t) = \theta_{\mathrm{m,i-1}} + \omega_{\mathrm{m,i-1}}t + \frac{1}{2}a_{\mathrm{m,i-1}}t^2 + \frac{1}{6}j_{\mathrm{m,i}}t^3, \tag{11a}$$

$$\omega_{\mathrm{m,i}}(t) = \omega_{\mathrm{m,i-1}} + a_{\mathrm{m,i-1}}t + \frac{1}{2}j_{\mathrm{m,i}}t^2, \tag{11b}$$

$$a_{\mathrm{m,i}}(t) = a_{\mathrm{m,i-1}} + j_{\mathrm{m,i}}t, \tag{11c}$$

where $i = \{1, 2, \ldots, 7\}$ denotes the specific phase under consideration. With reference to Fig. 5, based on the four parameters t_{a}, t_{d}, ω_1, ω_2 mentioned above, we first introduce the following "acceleration" and "deceleration" jerk values

$$j_{\mathrm{a}} = \frac{\omega_1}{2/9t_{\mathrm{a}}^2}, \quad j_{\mathrm{d}} = \frac{\omega_1 - \omega_2}{10/21t_d^2}, \tag{12}$$

and then the reference is generated as follows:

- The acceleration phase is divided in three intervals $I_{01} = [t_0, t_1]$, $I_{12} = [t_1, t_2]$, $I_{23} = [t_2, t_3]$ of equal lengths $|I_{01}| = |I_{12}| = |I_{23}| = \frac{1}{3}t_\mathrm{a}$ with constant jerks j_a, 0, $-j_\mathrm{a}$ as in (12), so that one obtains from (11) $\omega_\mathrm{m}(t_\mathrm{a}) = \omega_\mathrm{m}(t_3) = \omega_1$.
- The "sliding" interval $I_{34}=[t_3, t_4]$ is executed with constant speed ω_1 and length $|I_{34}|=T_\mathrm{slide}$, defined below.
- The deceleration phase is characterized by a short interval $I_{45} = [t_4, t_5]$ with $|I_{45}| = \frac{1}{21}t_\mathrm{d}$ having a constant negative jerk $-20j_\mathrm{d}$ followed by a longer phase $I_{56} = [t_5, t_6]$ with $|I_{56}| = \frac{20}{21}t_\mathrm{d}$ and positive jerk j_d; with the choice in (12), one gets from (11) $\omega_\mathrm{m}(t_6) = \omega_2$ and $a_\mathrm{m}(t_6) = 0$.
- The final approaching phase $I_{67} = [t_6, t_7]$ has length $|I_{67}| = T_\mathrm{end}$ (defined below) that ensures $\theta_\mathrm{m}(t_7) - \theta_\mathrm{m}(t_6) = \theta_\mathrm{f}$.

In summary, the following jerk values are imposed, with times $t_0 < t_1 < \cdots < t_7$ as shown in Fig. 5:

$$j(t) = \begin{cases} j_\mathrm{a} & \text{if } t_0 < t \le t_1, \\ 0 & \text{if } t_1 < t \le t_2,\ t_3 < t \le t_4,\ t_6 < t \le t_7, \\ -j_\mathrm{a} & \text{if } t_2 < t \le t_3, \\ -20j_\mathrm{d} & \text{if } t_4 < t \le t_5, \\ j_\mathrm{d} & \text{if } t_5 < t \le t_6, \end{cases}$$

Then, the reference values $r(t) = (r_\theta(t), r_\omega(t), r_a(t)) = (\theta^*_\mathrm{m}(t),\ \omega^*_\mathrm{m}(t),\ a^*_\mathrm{m}(t))$ can be computed from (11) after imposing the continuity conditions. The duration of the constant speed sections I_{34} and I_{67} can be obtained as follows

$$T_\mathrm{end} = \frac{\theta_\mathrm{f}}{\omega_2}, \quad T_\mathrm{slide} = \frac{\theta_\mathrm{tot} - \theta_\mathrm{a} - \theta_\mathrm{d} - \theta_\mathrm{f}}{\omega_1}, \tag{13}$$

where θ_tot is the total displacement of the gate, θ_a and θ_d denote the space covered in the acceleration and deceleration phases, respectively. The feedforward term u_ff is defined as a function of the reference $r = (r_\theta, r_\omega, r_a)$ and is introduced to improve the control accuracy and the response speed. To select u_ff, we first consider the linearized plant model given by eqs. (1), (6). Since the electrical time constant of the motor is much smaller than the mechanical time constant, the dynamics of the current can be ignored for the feedforward generation. Therefore, by imposing $L_\mathrm{a}\frac{di_a(t)}{dt} = 0$, along the reference motion r, equation (1) becomes

$$0 = -R_\mathrm{a} i_\mathrm{a} - k_\mathrm{t} r_\omega + u_\mathrm{ff}, \tag{14}$$

which provides $i_\mathrm{a} = \frac{u_\mathrm{ff} - k_\mathrm{t} r_\omega}{R_\mathrm{a}}$. Substituting this expression in (6), we obtain the simplified mechanical model

$$\dot{r}_\omega = -\left(\frac{k_\mathrm{t}^2 + R_\mathrm{a} b_\mathrm{tot}}{R_\mathrm{a} J_\mathrm{tot}}\right) r_\omega + \frac{k_\mathrm{t}}{R_\mathrm{a} J_\mathrm{tot}} u_\mathrm{ff} - \frac{\tau_\mathrm{c}}{J_\mathrm{tot}}\mathrm{sign}(r_\omega), \tag{15}$$

where r_ω denotes the reference speed. It is readily seen that a suitable feedforward action (a right inverse of (15)) is

$$u_\mathrm{ff} = \frac{R_\mathrm{a} J_\mathrm{tot}}{k_\mathrm{t}} r_a + \left(\frac{k_\mathrm{t}^2 + R_\mathrm{a} b_\mathrm{tot}}{k_\mathrm{t}}\right) r_\omega + \frac{R_\mathrm{a}}{k_\mathrm{t}}\tau_\mathrm{c}\mathrm{sign}(r_\omega). \tag{16}$$

Indeed replacing (16) in (15) one obtains $\dot{r}_\omega = r_a$, as desired.

IV. Robust feedback control design

We design a robust feedback control action using an optimization algorithm that aims to guarantee the stability, to shape the transient performance by constraining the closed-loop eigenvalues in a region of the left half-plane and to optimize a linear quadratic performance index. Considering the optimized solutions of the simplified model (15), and defining the error vector $e = [e_\theta\ \ e_\omega]^\top = [r_\theta - y_\theta\ \ r_\omega - y_\omega]^\top \in \mathbb{R}^2$, the error dynamics follows:

$$\dot{e} = Ae + Bu_\mathrm{fb} = \begin{bmatrix} 0 & 1 \\ 0 & -\left(\frac{k_\mathrm{t}^2}{R_\mathrm{a} J_\mathrm{tot}} + \frac{b_\mathrm{tot}}{J_\mathrm{tot}}\right) \end{bmatrix} e + \begin{bmatrix} 0 \\ -\frac{k_\mathrm{t}}{R_\mathrm{a} J_\mathrm{tot}} \end{bmatrix} u_\mathrm{fb}. \tag{17}$$

Some elements involved in the system matrices A and B may be uncertain or time varying. Then, we can express (17) as a function of the uncertain terms that are grouped in a vector p

$$\dot{e} = A(p)e + B(p)u_\mathrm{fb}. \tag{18}$$

We consider that each uncertain parameter p_i is bounded between a minimum and a maximum value $\underline{p_i}$ and $\overline{p_i}$, namely $p_i \in [\underline{p_i},\ \overline{p_i}]$, and we select $p_1 = \frac{1}{J_\mathrm{tot}}$ and $p_2 = \frac{1}{R_\mathrm{a} J_\mathrm{tot}}$. In this case study, we consider that the resistance R_a and the total inertia J_tot are uncertain parameters. The components of the parameter vector p are restricted inside the following intervals

$$p_1 \in [1/J_\mathrm{tot,M},\ 1/J_\mathrm{tot,m}], \tag{19a}$$

$$p_2 \in [1/(R_\mathrm{a,M} J_\mathrm{tot,M}),\ 1/(R_\mathrm{a,m} J_\mathrm{tot,m})], \tag{19b}$$

where $R_{\mathrm{a,m}}$, $J_{\mathrm{tot,m}}$, $R_{\mathrm{a,M}}$ and $J_{\mathrm{tot,M}}$ are the minimum and maximum values of the model parameters. Since A and B depend linearly on the uncertain vector p, a polytope of $n = 4$ vertices that contains all the possible values of the uncertain matrices can be defined characterized by matrices A_j and B_j, with $j = 1, \ldots, n$. For an extensive explanation of polytopic models of uncertainty see [11].

The feedback control law is given by

$$u_{\mathrm{fb}} = Ke = \begin{bmatrix} k_p & k_d \end{bmatrix} e, \tag{20}$$

where K is selected to place closed-loop poles in the complex plane in the intersection of three elementary LMI regions: an α-stability region, a disk of radius ρ, and a conic sector determined by ϑ. Also, the optimal LQR problem consists in finding a control input for (17) that minimizes the integral cost

$$J = \int_0^\infty e^\top Q\, e + u_{\mathrm{fb}}^\top R\, u_{\mathrm{fb}}, \tag{21}$$

where Q and R are symmetric positive-definite matrices. Fixing parameters $\alpha \geq 0$, $\rho > \alpha$, $\vartheta \in [0, \pi/2]$, the LQR controller is found by solving the optimization problem

$$\max_{\substack{\beta \in \mathbb{R},\, W \in \mathbb{R}^{2\times 2}, \\ X \in \mathbb{R}^{1\times 2}}} \beta \quad \text{subject to:}$$

$$W = W^\top > 0 \tag{22a}$$

$$\beta I - W < 0 \tag{22b}$$

$$M + M^\top + 2\alpha W < 0 \tag{22c}$$

$$\begin{bmatrix} (M+M^\top)\sin(\vartheta) & (M-M^\top)\cos(\vartheta) \\ (M^\top - M)\cos(\vartheta) & (M+M^\top)\sin(\vartheta) \end{bmatrix} \leq 0 \tag{22d}$$

$$\begin{bmatrix} -\rho W & M^\top \\ M & -\rho W \end{bmatrix} \leq 0 \tag{22e}$$

$$\begin{bmatrix} M+M^\top & W & X^\top \\ W & -Q^{-1} & 0 \\ X & 0 & -R^{-1} \end{bmatrix} < 0, \tag{22f}$$

$$M_j + M_j^\top < 0, \;\; j = 1, \ldots, n, \tag{22g}$$

where $M := A_0 W + B_0 X$ is defined by the nominal model A_0 and B_0, while $M_j := A_j W + B_j X$ represent the vertices A_j and B_j of the uncertainty polytope. Constraints (22c), (22d), (22e) shape the region of the complex plane, modifying the dynamical properties of the system, while constraints (22b), (22f) optimize the linear quadratic index (21). Constraint (22g) guarantees stability of the error dynamics in the presence of model uncertainty.

Proposition 1. *Selecting $\alpha \geq 0$, $\vartheta \in [0, \pi/2]$ and $\rho > \alpha$, for any feasible solution to (22), selecting $K = XW^{-1}$ the following properties hold: i) the closed-loop matrix $(A_j + B_j K)$ has eigenvalues with absolute value less than ρ, ii) the damping factor of the poles is larger than $\cos(\vartheta)$, iii) for all p in the uncertainty polytope, $(A_j(p) + B_j(p)K)$ has eigenvalues with real part smaller than $-\alpha$, iv) the LQR cost satisfies $J \leq \beta^{-1}|e(0)|^2$ along all solutions.*

Proof. i-iii) See the results in [6, Proposition 3].
iv) Performing a Schur-complement twice on (22f) we obtain

$$M + M^\top + WQW + X^\top R X < 0. \tag{23}$$

Substituting $M = AW + BX$, $X = KW$ and left-right multiplying by $e^\top$ we get

$$e^\top (A_{cl} W + W A_{cl}^\top) e + e^\top Q e + u^\top R u < 0 \;\; \forall e \neq 0. \tag{24}$$

where $A_{cl} = A + BK$ and $u = Ke$. Defining $V(e) = e^\top P e$ with $P = W^{-1}$ and noting that (24) implies that $A_{cl} W + W A_{cl}^\top < 0$ and that $e(t)$ converges to zero as $t \to \infty$, we may integrate (24) between 0 and T and take the limit as $T \to \infty$ to obtain

$$J < \int_0^\infty \frac{d}{dt} V(e(\tau)) d\tau = V(e(0)) = e(0)^\top P e(0). \tag{25}$$

Hence, by using constraint (22b) we can ensure that

$$J = e(0)^\top P e(0) = e(0)^\top W^{-1} e(0) \leq \beta^{-1} |e(0)|^2. \tag{26}$$

□

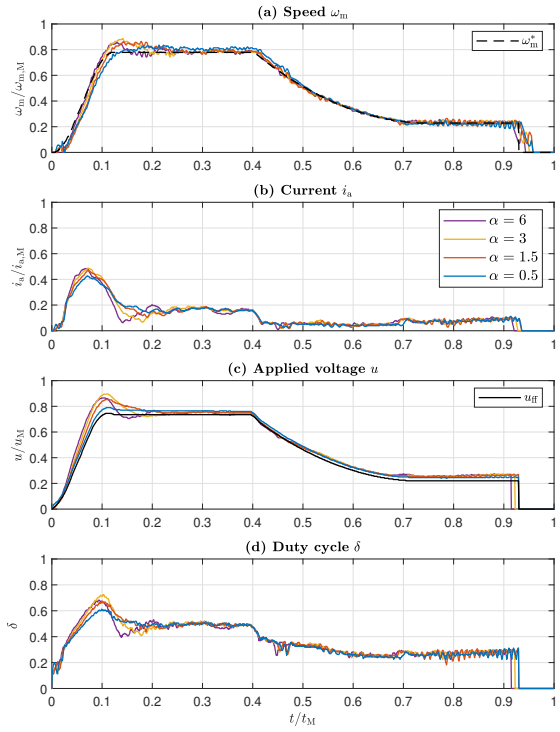

Fig. 6. Experimental responses of the gate automation using the proposed two-degree-of-freedom control for different values of the tuning parameter α. (a) motion reference ω_{m}^* and speed ω_{m}; (b) motor current i_{a}; (c) control input u and (d) duty cycle δ obtained from the feedback linearization. Constants $\omega_{\mathrm{m,M}}$, $i_{\mathrm{a,M}}$, u_{M} and t_{M} are normalization factors.

For this application, we choose a matrix Q to penalize the speed error, while R is used to avoid large sizes of K. This choice induces desirable results, as illustrated in the next Section. It is worth to point out that while solving the LMI optimization problem (22) requires the use of convex optimization tools, once the controller gains are determined, the implementation of the proposed solution in a real embedded control system does not require more computational effort than a classical control scheme. Moreover, one of the main advantages with this formulation is to include uncertainties in the feedback gain selection, while classical LQR control is only valid for systems without uncertainty.

V. Experimental Results

In order to verify the results derived in the previous sections we implemented the proposed control strategy in an industrial electric gate. Specifically, the controller has been written in C language and implemented on a 8-bit microcontroller (Microchip PIC18F device) mounted on a control board provided by the company developing the application. In Fig. 6, we show the set of responses of the closed loop system obtained by varying the tuning parameter α of the LMI optimization. Increasing the values of α results in better tracking of the reference, especially in the acceleration phase. However, a larger overshoot can be observed at the end of the acceleration phase, due to the larger feedback gains. Note also that the reference is badly followed at the start of the maneuver, probably due to the significant mechanical backlash of the transmission system. The reference motion was validated by testing different user settable parameter values. Compared to the trapezoidal trajectory characterized by an impulsive jerk profile, the adopted motion profile has limited jerk and attenuates the excessive stresses generated by the step variations of acceleration on the actuators and on the mechanical structure, thus extending the useful life of the device. In Fig. 7 the robustness of the proposed controller (with $\alpha = 1.5$) is tested for a model parameter uncertainty. Specifically, the mass of the physical gate has been changed to have a variation of the total inertia of ± 25 percent with respect to the nominal inertia J_{tot}. It can be noted that, while the input actions δ and u increase or decrease to compensate for the different inertia, the outputs remain similar thereby showing successful feedback action. Finally, the response of the proposed controller (with $\alpha = 1.5$) is compared with the one of the production standard controller in Fig. 8, resulting in a significant improvement of the tracking performance. The production controller is a PI speed controller, manually tuned by adjusting the gains until acceptable results are obtained. In Fig. 8(c) it can be also observed that the applied voltage for the proposed controller does not saturate as it remains always within its minimum and maximum values, computed using (10).

VI. Conclusions

In this paper, a control architecture for an electric gate is proposed. The nonlinear dynamics of the motor drive is compensated by a feedback linearization action, the feedforward input is computed as a function of a smooth speed reference signal, and

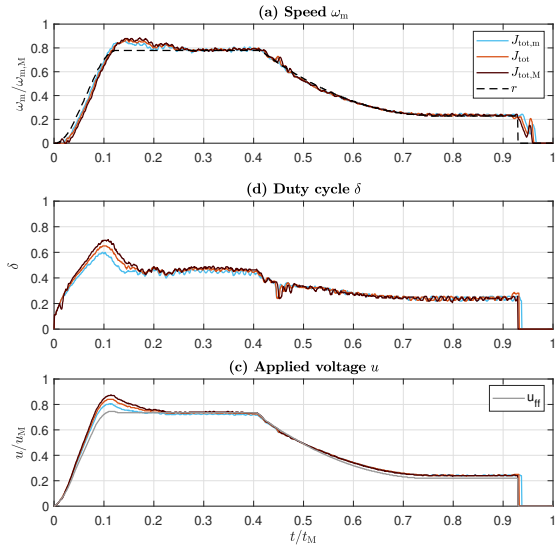

Fig. 7. Experimental output (a) and input (b) in the presence of a load inertia perturbation of $\pm 25\%$.

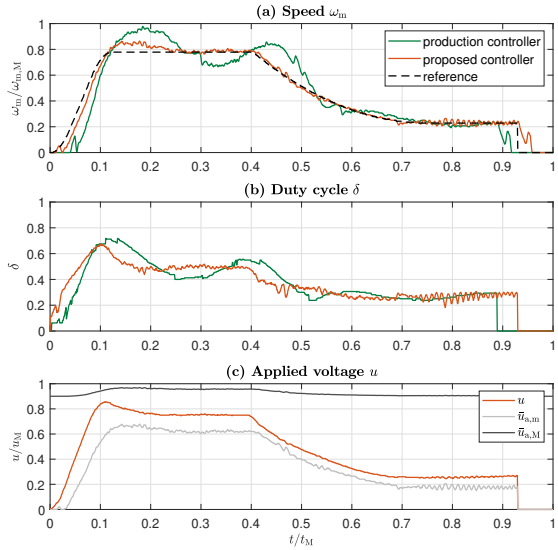

Fig. 8. Comparison between the performance of the proposed controller and the production standard controller.

a robust feedback controller is tuned using LMI optimization. The effectiveness of this approach has been illustrated with experimental tests carried out on a prototype device. Future work may include explicit consideration of the saturation in the control algorithm and the implementation of adaptive control techniques to eliminate systematic errors in the trajectory tracking task, in addition to alternative feedback control architectures, such as a conventional P-PI cascade with a P position controller and an underlying PI speed controller.

REFERENCES

[1] S. E. Lyshevski, *Electromechanical systems, electric machines, and applied mechatronics*. CRC press, 2018.

[2] R. Crowder, *Electric drives and electromechanical systems: applications and control*. Butterworth-Heinemann, 2019.

[3] P. Lambrechts, M. Boerlage, and M. Steinbuch, "Trajectory planning and feedforward design for electromechanical motion systems," *Control Engineering Practice*, vol. 13, no. 2, pp. 145–157, 2005.

[4] A. Hughes and B. Drury, *Electric motors and drives: fundamentals, types and applications*. Newnes, 2019.

[5] G. C. Ioannidis, C. Psomopoulos, S. Kaminaris, P. Pachos, H. Villiotis, S. Tsiolis, P. Malatestas, G. Vokas, and S. Manias, "AC-DC & DC-DC converters for DC motor drives," in *Proc. of the International Conf. on Electronics and Communication Systems*, vol. 2, 2013.

[6] D. Cunico, A. Cenedese, L. Zaccarian, and M. Borgo, "Nonlinear modeling and feedback control of boom barrier automation," *arXiv:2109.13291*, 2021.

[7] A. Gasparetto and V. Zanotto, "A technique for time-jerk optimal planning of robot trajectories," *Robotics and Computer-Integrated Manufacturing*, vol. 24, no. 3, pp. 415–426, 2008.

[8] Y. Fang, J. Hu, W. Liu, Q. Shao, J. Qi, and Y. Peng, "Smooth and time-optimal S-curve trajectory planning for automated robots and machines," *Mechanism and Machine Theory*, vol. 137, pp. 127–153, 2019.

[9] H. Wang, H. Wang, J. Huang, B. Zhao, and L. Quan, "Smooth point-to-point trajectory planning for industrial robots with kinematical constraints based on high-order polynomial curve," *Mechanism and Machine Theory*, vol. 139, pp. 284–293, 2019.

[10] K. D. Nguyen, T.-C. Ng, and I.-M. Chen, "On algorithms for planning s-curve motion profiles," *International Journal of Advanced Robotic Systems*, vol. 5, no. 1, p. 11, 2008.
[11] S. Boyd, L. El Ghaoui, E. Feron, and V. Balakrishnan, *Linear matrix inequalities in system and control theory*. SIAM, 1994.
[12] C. Olalla, R. Leyva, A. El Aroudi, and I. Queinnec, "Robust LQR control for PWM converters: An LMI approach," *IEEE Transactions on industrial electronics*, vol. 56, no. 7, pp. 2548–2558, 2009.
[13] M. Ge, M.-S. Chiu, and Q.-G. Wang, "Robust PID controller design via LMI approach," *Journal of process control*, vol. 12, pp. 3–13, 2002.
[14] M. Chilali and P. Gahinet, "$\mathcal{H}_\infty$ design with pole placement constraints: an LMI approach," *IEEE Transactions on Automatic Control*, vol. 41, pp. 358–367, 03 1996.
[15] R. Krishnan, *Electric motor drives: modeling, analysis and control*. Prentice Hall, 2001.